tests are used (*21*), suggests that an average explosive volcanic cloud height of at least 7000 m would be involved to yield a dominant particle size of 50 μm or less at a distance of 600 km.

Preliminary results of detailed particle size analyses of the atmospherically transported volcanic dust and micropumice fragments in the cores are now available (*13*), and they support completely our inference of a downwind decrease in volcanic dust concentrations which, according to examination by binocular and transmitted light microscopy, are unaltered by any seafloor processes.

Windom's (*22*) proposal that deep-sea sediments may contain large fractions of windblown materials is supported by our data, which further suggest that one may map the contribution from suspected volcanic sources by measuring magnetic properties of cores from traverses or grids focused on the source region. Furthermore, such data can be rapidly obtained from cores in unsplit plastic liners.

W. KENNETH FREED
NORMAN D. WATKINS
Graduate School of Oceanography, University of Rhode Island, Kingston

References and Notes

1. A. Cox, R. R. Doell, by G. B. Dalrymple, *Science* **144**, 1537 (1964); I. McDougall and F. H. Chamalaun, *Nature (Lond.)* **212**, 1415 (1966).
2. M. J. Keen, *Deep-Ses Res.* **10**, 607 (1963); C. G. A. Harrison, *J. Geophys. Res.* **71**, 3033 (1966).
3. Summarized by N. D. Watkins in *Geol. Soc. Am. Bull.* **83**, 551 (1972).
4. N. D. Opdyke, B. Glass, J. D. Hays, J. Foster, *Science* **154**, 349 (1966); N. D. Watkins and H. G. Goodell, *Earth Planet. Sci. Lett.* **2**, 123 (1967).
5. N. D. Opdyke, *Rev. Geophys. Space Phys.* **10**, 213 (1972); C. G. A. Harrison, *Earth-Sci. Rev.* **10**, 1 (1974).
6. C. Amerigian, *Earth Planet. Sci. Lett.* **21**, 321 (1974).
7. N. D. Watkins, D. R. Kester, J. P. Kennett, *ibid.* **24**, 113 (1974).
8. R. Løvlie, W. Lowrie, M. Jacobs, *ibid.* **15**, 157 (1971).
9. D. V. Kent and W. Lowrie, *J. Geophys. Res.* **79**, 2987 (1974).
10. S. E. Haggerty, *Carnegie Inst. Washington Yearb.* **68**, 332 (1970).
11. W. I. Ridley, N. D. Watkins, D. J. MacFarlane, in *The Ocean Basins and Margins*, A. E. M. Nairn and F. G. Stehli, Eds. (Plenum, New York, 1973), vol. 2, pp. 445–483. All distances in the present study are measured from San Jorge Island.
12. B. H. Corliss, thesis, University of Rhode Island (1973).
13. T.-C. Huang, W. K. Freed, B. H. Corliss, *Geol. Soc. Am. Abstr. Programs* **6**, 801 (1974).
14. L. Molyneux, *Geophys. J. R. Astron. Soc.* **24**, 429 (1971).
15. ———, R. Thompson, F. Oldfield, M. E. McCallan, *Nat. Phys. Sci.* **237**, 42 (1972).
16. Bison Instruments magnetic susceptibility system model 3200, modified for the measurement of long cores by means of a pull-through coil attachment.
17. T. J. Smayda, *Mar. Geol.* **11**, 105 (1971); J. W. Pierce and B. O. Myers, *Geol. Soc. Am. Abstr. Programs* **6**, 388 (1974).
18. T.-C. Huang, N. D. Watkins, D. M. Shaw, *Geol. Soc. Am. Bull.*, in press.
19. R. F. King and A. I. Rees, *J. Geophys. Res.* **71**, 561 (1966).
20. D. M. Shaw, N. D. Watkins, T.-C. Huang, *ibid.* **79**, 3087 (1974).
21. B. R. Morton, G. Taylor, J. S. Turner, *Proc. R. Soc. Ser. A Math. Phys. Sci.* **234**, 1 (1956).
22. H. L. Windom *Geol. Soc. Am. Bull.* **80**, 761 (1969).
23. This research is supported by NSF grants GA 28853 and DES 74-22347.

17 December 1974; revised 4 March 1975

Structure of Coat Proteins in Pf1 and fd Virions by Laser Raman Spectroscopy

Abstract. *Raman spectra of filamentous bacterial viruses are dominated by scattering from vibrations of the protein capsomers. The amino acid compositions of coat proteins in Pf1 and fd strains are recognized by their different side-chain vibrational frequencies. However, the conformationally sensitive amide frequencies indicate that Pf1 and fd coat proteins have the same α-helical secondary structures. Viral DNA backbones do not exhibit the A-type geometry.*

A molecular model of filamentous bacterial viruses has been proposed on the basis of low resolution x-ray diffraction data (*1, 2*). Since details of the structure at the atomic level cannot be resolved by the x-ray data, it is essential to support the model by other lines of evidence. Using laser Raman spectroscopy, we present here the results of a study of protein and nucleic acid secondary structures in these viruses.

The method depends on the ability to obtain by laser light scattering a vibrational spectrum, consisting of a series of lines or frequencies characteristic of the structure and environment of macromolecular subgroups (*3*). Applications to nucleic acids (*4*) utilize the dependence of Raman frequencies and intensities on the amount and kind of base and backbone interactions to quantify RNA (*5*) and DNA (*6*) secondary structures. Applications to proteins (*7*) make use of the conformationally sensitive amide frequencies to distinguish α, β, and random-chain regions of the polypeptide backbone. Raman spectroscopy may also be applied to more complex assemblies, such as virions, to investigate stabilizing interactions of nucleic acid and protein (*8*). Information of high structural specificity is usually difficult to obtain on such systems by other techniques, particularly when water is used as a solvent.

We report here the Raman spectra of aqueous solutions of the filamentous bacterial (FB) viruses, Pf1 and fd strains. These are the first Raman spectra obtained on true DNA-protein complexes and are unusual for their high signal-to-noise quality and rich patterns of Raman lines.

The FB viruses are of considerable interest (*2*). Both Pf1 and fd are linear assemblies (19,500 Å and 9,000 Å, respectively, in length by 60 Å in diameter) of coat protein subunits encapsulating a DNA molecule. The DNA, which comprises not more than 12 percent by weight of either virion, is believed to be a circular single strand. The major coat protein in both strains comprises about 99 percent of all the viral protein, has a molecular weight of about 5000, and is believed to be largely α-helical in structure (*1, 2*). Primary structures of the major coat proteins in Pf1 and fd are, however, different (*1, 2, 9*). Proline, tryptophan, glutamic acid, and phenylalanine are absent from Pf1 but are present in fd, while glutamine and arginine are present in Pf1 but absent from fd.

Pf1 and fd were obtained and purified as described (*10*). For Raman spectroscopy solutions were prepared in 0.05*M* NaCl at *p*H 9. Spectra were excited with 488.0- and 514.5-nm lines of an argon-ion laser (Coherent Radiation Laboratories) and were recorded on a Ramalog spectrometer (Spex Industries, Inc.). Samples were contained in 1.0-mm capillary tubes and held at constant temperature as described (*11*).

All spectra were reproducible over a period of 48 hours, and changes in the spectra as a function of temperature were reversible over the range 32° to 75°C. Assays showed no loss of viral activity due to laser illumination or other sample handling.

The Raman data as recorded are shown in Fig. 1. Unusually high signal-to-noise ratios were obtained with both Pf1 and fd despite the noticeable background fluorescence in the latter case. The fluorescence is attributed to a viral component and not to impurities in the fd preparation. The spectra of both Pf1 and fd are dominated by Raman scattering of the coat protein in the regions 200 to 1800 cm^{-1} and 2800 to 3100 cm^{-1}.

Recent Raman studies of aqueous proteins and polypeptides (*7, 12, 13*) indicate the following. Helical structures give a strong and sharp amide I line at 1650 ± 5 cm^{-1} and relatively weak scattering in the amide III region (1265 to 1300 cm^{-1}). β-Structures give a strong and sharp amide I line at 1665 ± 5 cm^{-1} and a strong amide III line at 1235 ± 10 cm^{-1}. Random structures give a strong but broad amide I line at about 1665 cm^{-1} and a medium amide III line at 1248 ± 5 cm^{-1}. Therefore, the amide frequencies and intensities in Fig. 1 confirm that the coat proteins of Pf1 and fd have the same α-helical secondary structures. Furthermore, the absence of additional Raman scattering in the amide I region, which could be assigned to β or random structures, indicates that the coat proteins are uniformly α-helical (*14*). Weak Raman scattering near 1685 cm^{-1} in the spectra of Fig. 1 is attributed to the carbonyl stretching vibrations of the DNA bases (*3–6*).

Supporting evidence for the α-helical secondary structures of Pf1 and fd coat proteins is also found in the low-frequency region of the Raman spectrum. For example, both Pf1 and fd exhibit lines near 377 and 530 cm^{-1} which are assignable to alanine residues in the right-handed α-helical conformation (*15*).

The amide I line of Pf1 appears at 1652 cm^{-1} when the temperature is 32°C (Fig. 1) and is shifted to 1655 cm^{-1} at 50°C and to 1657 cm^{-1} at 75°C with no change in half-width. Upon being cooled to 32°C, amide I returns to a frequency of 1652 cm^{-1}. The same reversible frequency shift is observed for amide I of fd coat protein. Increasing the temperature of Pf1 or fd also causes a significant increase in the Raman intensity at 377 cm^{-1}, so that at 75°C, the lines at 337 and 377 cm^{-1} have equal peak heights. These effects indicate that the α-helical structures are altered reversibly by changes in temperature over the range 32° to 75°C. Such modification of the coat protein structure occurs, however, without impairment of viral activity (*9*), and suggests considerable flexibility in the FB virion. We note also that 3 percent solutions of Pf1 or fd give amide I lines at 1649 cm^{-1}. This frequency difference indicates, however, a spectral distortion caused by the overlapping water band (1640 cm^{-1}) rather than by a solvent-induced structural perturbation.

Since DNA accounts for not more than 12 percent by weight of the virion, its Raman scattering is weak in comparison to that of the coat protein. Nevertheless, the spectra of Fig. 1 are informative with regard to DNA structure. A-DNA gives a Raman line at 810 cm^{-1} with intensity equal to that of the pyrimidine line at 785 cm^{-1} (*6*). In Pf1 there is no Raman line between 790 and 825 cm^{-1} despite the clearly resolved pyrimidine line at 785 cm^{-1}. In fd the line at 801 cm^{-1} is too weak in intensity and too low in frequency to be assigned to the A-DNA vibration, but it is easily accounted for by scattering expected of amino acid residues near this frequency. Therefore the DNA backbone in Pf1 and fd virions cannot be in the A-configuration (*16*). Since B-DNA and C-DNA give no prominent Raman line between 790 and 825 cm^{-1} (*6*), data of Fig. 1 are consistent with a backbone geometry of either type.

We cannot determine from our results whether hydrogen bonding interaction occurs between base residues opposite one another in the encapsulated DNA strand. However, the pyrimidine line at 785 cm^{-1} and the purine line near 1580 cm^{-1} exhibit sufficiently low intensities so that it is possible that considerable stacking of the DNA base residues occurs (*3–5*). These intensities, moreover, do not increase significantly when the viruses are heated to 75°C.

Finally, Fig. 1 demonstrates the ability to distinguish two closely related DNA coliphages from one another on the basis of their Raman vibrational spectra. The presence of phenylalanine in fd coat protein, for example, leads to the appearance of strong lines at 620 and 1004 cm^{-1}, additional strong scattering at 1206, 1488, 1608, and 3060 cm^{-1}, and other weaker lines characteristic of the phenylalanine residue, all of which are absent from the

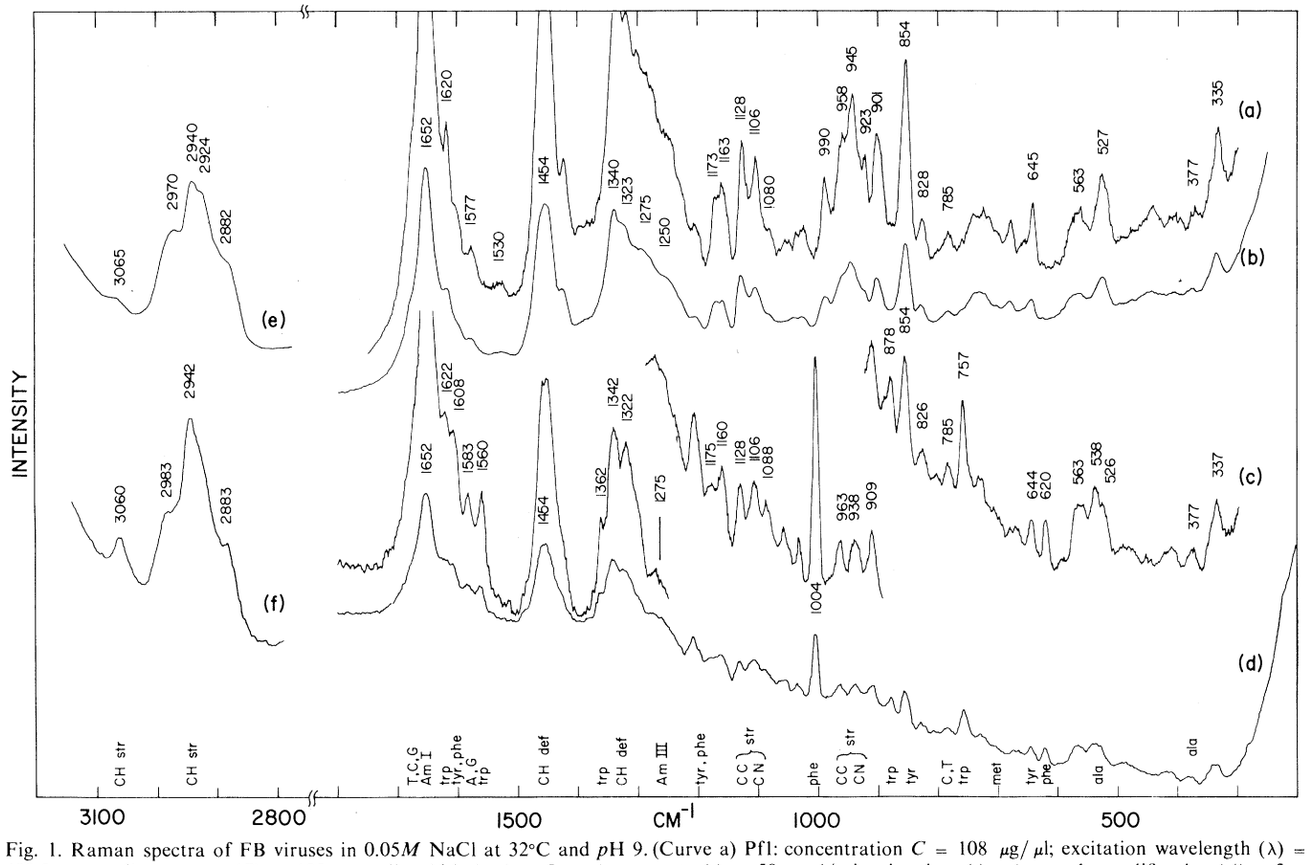

Fig. 1. Raman spectra of FB viruses in 0.05*M* NaCl at 32°C and *p*H 9. (Curve a) Pf1: concentration C = 108 $\mu g/\mu l$; excitation wavelength (λ) = 488.0 nm; radiant power (P) = 100 mw; slit width ($\Delta\sigma$) = 5 cm^{-1}; scan rate (r) = 50 cm^{-1}/min; rise time (t) = 1 second; amplification (A) = 3×. (Curve b) Pf1: $\Delta\sigma$ = 10 cm^{-1}; t = 3 seconds; A = 1×; other conditions as in (a). (Curve c) fd: C = 147 $\mu g/\mu l$; λ = 514.5 nm; P = 100 mw; $\Delta\sigma$ = 5 cm^{-1}; r = 50 cm^{-1}/min; t = 1 second; A = 3×. (Curve d) fd: $\Delta\sigma$ = 9 cm^{-1}; t = 3 seconds; A = 1×; other conditions as in (c). (Curve e) Pf1: A = ⅓×; other conditions as in (b). (Curve f) fd: A = ⅓×; other conditions as in (d). Frequencies of prominent lines are given in cm^{-1} units and assignments to molecular subgroups are denoted by standard abbreviations (*17*). Abbreviations: str, stretching; def, deformation; CH, carbon-hydrogen bond; CC, carbon-carbon bond; CN, carbon-nitrogen bond; A, T, C, and G, adenine, thymine, cytosine, and guanine; ala, alanine; met, methionine; phe, phenylalanine; trp, tryptophan; tyr, tyrosine; Am, amide.

spectrum of Pf1. Tryptophan is distinguished in fd by its Raman lines at 757, 878, 1012, 1362, and 1560 cm^{-1}, while proline and glutamic acid account for the lines of fd at 415 and 670 cm^{-1}. Conversely, the lines of Pf1 at 405, 444, 520, 655, and 945 cm^{-1} may be attributed to glutamine and arginine residues. As in the case of R17 phage (*8*), the CH-stretching (2800 to 3100 cm^{-1}) and CH-deformation (1320 to 1460 cm^{-1}) regions are dominated by contributions from the -CH, $-CH_2-$, and $-CH_3$ groups of amino acid side chains (*17*).

In summary, the Raman data indicate the following features of FB virus structure. The coat proteins of Pf1 and fd virions have the same α-helical secondary structures. The α-helices undergo a reversible change in geometry over the temperature interval 32° to 75°C. At the higher temperatures in this range, α-helices are maintained but apparently with somewhat weaker intramolecular hydrogen bonding than occurs at lower temperatures. The DNA chain in the virion of Pf1 or fd maintains a configuration in which the local geometry of phosphodiester linkages is dissimilar to that found in A-DNA. The DNA bases are probably stacked but no information on base pairing has been obtained from the spectra. These features of viral DNA structure are not altered over the range 32° to 75°C.

The significant spectral differences between Pf1 and fd are due to the different amino acid compositions of their respective coat proteins. The Raman spectrum therefore provides a simple and straightforward means of detecting and distinguishing these closely related FB viruses.

G. J. THOMAS, JR.
P. MURPHY

Department of Chemistry,
Southeastern Massachusetts University,
North Dartmouth 02747

References and Notes

→ D. A. Marvin and E. J. Wachtel, *Nature (Lond.)* **253**, 19 (1975).
→ Y. Nakashima, R. L. Wiseman, W. Konigsberg, D. A. Marvin, *ibid.*, p. 68.
3. G. J. Thomas, Jr., in *Vibrational Spectra and Structure*, J. R. Durig, Ed. (Dekker, New York, in press), vol. 3.
4. K. A. Hartman, R. C. Lord, G. J. Thomas, Jr., in *Physico-Chemical Properties of Nucleic Acids*, J. Duchesne, Ed. (Academic Press, New York, 1973), vol. 2, p. 1.
5. G. J. Thomas, Jr., and K. A. Hartman, *Biochim. Biophys. Acta* **312**, 311 (1973).
6. S. C. Erfurth, E. J. Kiser, W. L. Peticolas, *Proc. Natl. Acad. Sci. U.S.A.* **69**, 938 (1972).
→ M. C. Chen and R. C. Lord, *J. Am. Chem. Soc.* **96**, 4750 (1974).
→ K. A. Hartman, N. Clayton, G. J. Thomas, Jr., *Biochem. Biophys. Res. Commun.* **50**, 942 (1973).
9. D. A. Marvin and B. Hohn, *Bacteriol. Rev.* **33**, 172 (1969).
→ D. A. Marvin, R. L. Wiseman, E. J. Wachtel, *J. Mol. Biol.* **82**, 121 (1974). Our samples were provided by Professor D. A. Marvin.
→ G. J. Thomas, Jr., and J. R. Barylski, *Appl. Spectrosc.* **24**, 463 (1970).
→ T. J. Yu, J. L. Lippert, W. L. Peticolas, *Biopolymers* **12**, 2161 (1973).
→ B. G. Frushour and J. L. Koenig, *ibid.* **13**, 455 (1974).
14. We estimate that no more than 5 percent of the amino acid residues could exist in β regions without generating both a shoulder to the observed amide I line near 1665 cm^{-1} and a line in the amide III region near 1235 cm^{-1}. A nominally higher percentage of residues in randomly oriented regions would be allowed by our data.
→ K. Itoh, T. Hinomoto, T. Shimanouchi, *Biopolymers* **13**, 307 (1974).
→ L. A. Day, *J. Mol. Biol.* **39**, 265 (1969).
17. A complete list of the observed Raman frequencies and assignments of Pf1 and fd is available on request.
18. We thank Professor D. A. Marvin of Yale University for suggesting this project and providing samples of highly purified FB viruses. Supported by NSF grant GB 41382, NIH grant AI-11855-01, and a grant from the Research Corporation to G.J.T.; and by NIH grant CA-13094 to D. A. Marvin.

14 November 1974

Denudation Studies: Can We Assume Stream Steady State?

Abstract. *Contemporary stream sediment loads are dubious indicators of regional denudation. Recent analysis of ten river basins in the southeastern United States indicates that of the material eroded from upland slopes since European settlement, only about 5 percent has been exported. The remainder, alluvium and colluvium, will probably not be exported because of extensive reservoir impoundments.*

Stream steady state, wherein the solid material transported from stream basins is considered approximately equal to that eroded from upland slopes, cannot be assumed for much of the United States since European settlement (*1*). Sediment from culturally accelerated erosion has so overloaded streams that most of it has been deposited within the system. Thus, stream sediment loads, as used in most denudation studies (*2, 3*), are questionable indicators of regional denudation.

Analysis of ten large river basins, mostly within the southern Piedmont, indicates that of the material eroded from upland slopes since European settlement, only about 5 percent has been exported. Gross erosion (detached materials) was estimated from soil profile truncations (*4*), and sediment yields (export) were estimated from U.S. Geological Survey data (*5*) on suspended stream load with adjustments for bed load. Because of the varying length of agricultural occupancy of the basins, gross erosion and sediment yields were converted to standardized rates (Fig. 1); areally weighted, they average 95 and 4.5 mm per 100 years, respectively. Delivery

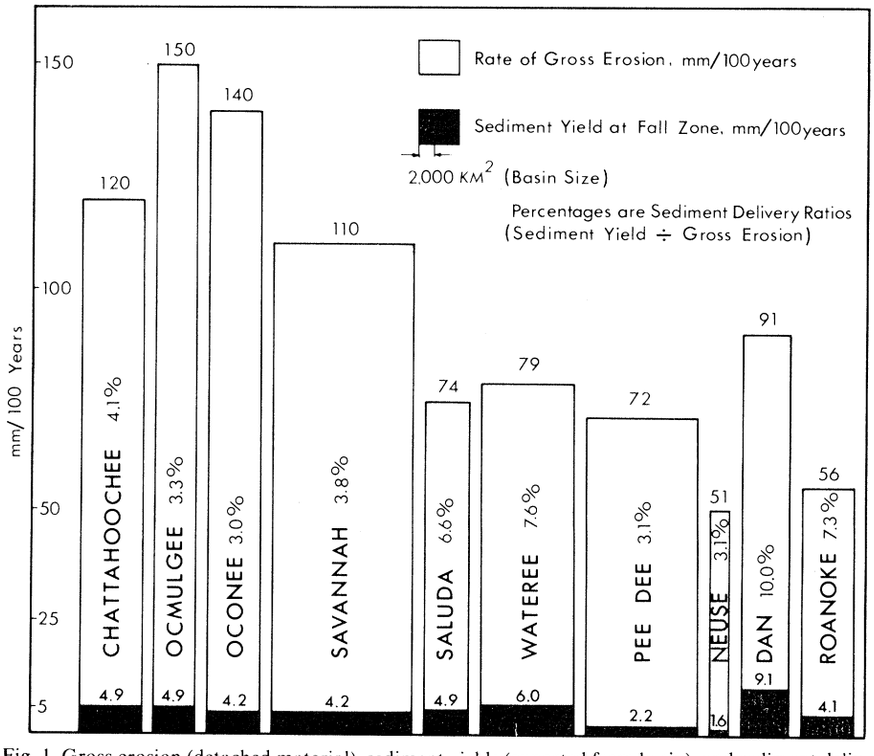

Fig. 1. Gross erosion (detached material), sediment yields (exported from basin), and sediment delivery ratios of selected southern Piedmont river basins since agricultural occupancy began. The areally weighted averages are: gross erosion, 95 mm per 100 years; sediment yield, 4.5 mm per 100 years; sediment delivery ratio, 4.7 percent.